A NEW ALGORITHMIC LIMIT CYCLE ANALYSIS METHOD FOR MULTIVARIABLE SYSTEMS*

James H. Taylor†

SUMMARY

The sinusoidal-input describing function (SIDF) technique is a well-known approach for studying limit cycle phenomena in nonlinear systems. In recent years, a number of extensions of the SIDF method have been developed to permit the analysis of systems with more than one nonlinearity. In general, the nonlinear system models that can be treated by such extensions have been quite restrictive (limited to a few nonlinearities, or to certain specific block diagram configurations). Furthermore, some results involve only conservative conditions for limit cycle avoidance, rather than actual limit cycle conditions. The technique described in this paper removes all constraints: Systems described by a general state vector differential equation, with any number of nonlinearities, may be analyzed. In addition, the nonlinearities may be multi-input, and bias effects can be treated. To the author's knowledge, this is the first instance of the SIDF limit cycle analysis of such systems.

The new SIDF methodology is fully developed in this paper, and its power and use are illustrated by application to a highly nonlinear model of a tactical aircraft in a medium angle-of-attack flight regime. Some problems associated with direct simulation (especially "obscuring modes" and the initial condition problem) are also discussed. Finally, combining the new technique with recent pole positioning methods based on state variable feedback is suggested as a very general way to approach multivariable nonlinear systems synthesis.

---

*This work was sponsored by the U.S. Office of Naval Research under Contract Number N00014-75-C-0432, and was first presented at a Roundtable Session at the IFAC Symposium on Multivariable Technological Systems, University of New Brunswick, Fredericton, N.B. Canada, July 1977.

†The Analytic Sciences Corporation, Reading, Massachusetts 01867.

1. INTRODUCTION

The study of limit cycle (LC) conditions in nonlinear systems is a problem of considerable interest in engineering. An approach to LC analysis that has gained widespread acceptance is the frequency domain/sinusoidal-input describing function (SIDF) methodology [1-4]. This technique, in simple terms, involves formulating the system as a feedback control system with single-input/single-output (SISO) linear dynamics $W(s)$ in the forward path and an SISO nonlinearity $f(e)$ in the return path. It is then assumed that the input e is sinusoidal, e.g., $e = a_0 \sin \omega t$, and the approximation

$$f(e) \cong \psi_1 \sin \omega t$$

$$\triangleq n_1(a_0) * a_0 \sin \omega t \qquad (1)$$

is made*. The fourier coefficient ψ_1 (and thus n_1) is generally complex (unless $f(e)$ is single-valued); the real and imaginary parts of ψ_1 represent the in-phase and quadrature fundamental components of $f(a_0 \sin \omega t)$, respectively. The so-called describing function $n_1(a_0)$ in (1) is "amplitude dependent", thus retaining a basic property of a nonlinear operation. By the principle of harmonic balance, the assumed oscillation -- if it is to exist -- must result in unity open-loop gain,

$$-W(j\omega)\, n_1(a_0) = 1 \qquad (2)$$

Condition (2) is easy to check using the polar or Nyquist plot of $W(j\omega)$ [1-4].

*If $f(e)$ is not odd ($f(-e) \neq -f(e)$), a constant term ("bias" or "D.C. value") must occur in (1); such cases present no difficulty [1-4], but are omitted to simplify the discussion.

It is generally well-understood that SIDF analysis as outlined above is only approximate, so caution is always recommended in its use. The standard caveats that $W(s)$ should be "low pass to attenuate higher harmonics" and that $f(e)$ should be "well-behaved*" (so that (1) is nearly true) indicate that the analyst has to be familiar with the system behavior, by direct experience or by simulation. Given an appreciation of these warnings, SIDF LC analysis has proven to be a very powerful engineering tool.

The utility of SIDF analysis for systems with one significant SISO nonlinearity has naturally resulted in a number of attempts to generalize the technique to the multiple-nonlinearity case. One generalization of the model described above is depicted in Fig. 1. The linear plant is modeled as a matrix of transfer functions $W(s)$ representing the dynamic relations between ℓ inputs (the vector $\underline{p}$) and m outputs (the vector $\underline{r}$). The output vector $\underline{r}$ is operated on by ℓ nonlinearities, the elements of $\underline{f}(\cdot)$, and the result is fed back in the standard negative feedback configuration (Fig. 1). For completeness, a bias input (possibly a fixed control vector $\underline{u}_0$) may be present.

When the multivariable nonlinear system model of Fig. 1 is treated with any configurational generality, e.g., neither W nor $\underline{f}$ are assumed to be diagonal, cf. [5,6], then the existing SIDF results are generally conservative conditions for limit cycle avoidance. Actual limit cycle conditions have been given only for specific restrictive configurations, e.g., a single closed loop of alternating linear dynamic blocks $W_i(s)$ and nonlinear characteristics $f_i(\cdot)$ [7,8,9], or a unity scalar feedback path around a forward path made up of a parallel network of the form $G_i(s)$ followed by $f_i(\cdot)$ followed by $H_i(s)$

*I.e., the first harmonic in (1) should be dominant in some sense.

[7,8,10], or for a rather small number of nonlinearities [11]. In every "multivariable" case reviewed by the author, only SISO nonlinearities were considered, and bias effects (either due to constant inputs $\underline{u}_0$ or to "rectification" caused by nonlinear effects) were excluded. The LC analysis approach described in this paper removes all restrictions with respect to model configuration, nonlinearity type, or the presence of biases.

The organization of the remainder of this paper is as follows: In Section 2 the need for more powerful SIDF LC analysis methods is motivated by outlining a system model representing aircraft dynamics in moderate angle-of-attack flight conditions for which available SIDF approaches are completely inadequate. The new approach to SIDF limit cycle analysis which permits very general nonlinear system models to be treated is presented in Section 3. In Section 4 the application of the new LC analysis method to the aircraft dynamics problem of Section 2 is illustrated, and direct simulation of the nonlinear equations of motion both as an SIDF analysis verification technique and as an LC study method in its own right is discussed. In Section 5 the status of the development of the new LC analysis technique and some preliminary conclusions about its efficacy are outlined.

2. A HIGHLY NONLINEAR AIRCRAFT DYNAMICS MODEL

In a realistic system model that represents the dynamics of a high-performance aircraft at moderate angle of attack, the analyst is confronted with a large number of nonlinearities. These nonlinearities arise in the characterization of both the empirical aerodynamic data for the specific aircraft (aerodynamic coefficients and stability derivatives) and dynamic and kinematic effects. The combined nonlinear

state equations for the aircraft motion can be written in body axes as in (3) if the generally small off-diagonal moment-of-inertia terms and non-axial thrust components are neglected [12].

$$\dot{\underline{x}} \triangleq \begin{bmatrix} \dot{\theta} \\ \dot{u} \\ \dot{q} \\ \dot{w} \\ \dot{v} \\ \dot{r} \\ \dot{p} \\ \dot{\phi} \end{bmatrix} = \begin{bmatrix} q \cos \phi - r \sin \phi \\ (X+T)/m + rv - qw - g \sin \theta \\ ((I_z - I_x)pr + M)/I_y \\ Z/m + qu - pv + g \cos \theta \cos \theta \\ Y/m + pw - ru + g \sin \phi \cos \theta \\ ((I_x - I_y)\, pq + N)/I_z \\ ((I_y - I_z)qr + L)/I_x \\ p + q \sin \phi \tan \theta + r \cos \phi \tan \theta \end{bmatrix} \triangleq \underline{f}(\underline{x}, \underline{u}) \qquad (3)$$

The state variables are the aircraft velocity components in body axes (u,v,w), the rotational rates about the body axes (p,q,r), and the pitch and roll Euler angles (θ,ϕ). The parameters g, m, I_x, I_y, I_z denote the acceleration due to gravity and the aircraft mass and moments of inertia.

Most of the dynamic and kinematic nonlinearities are expressed explicitly in (3), with terms that include products of states, states times trigonometric functions of states, and products of trigonometric functions of states. The aircraft data and response characteristics are associated with the force and moment components, X, Y, Z, L, M, N; these contributions are expressed in terms of non-dimensional aerodynamic force and moment coefficients as

$$X = \tfrac{1}{2}\rho V^2 S C_{X_T} \qquad L = \tfrac{1}{2}\rho V^2 S b C_{\ell_T}$$

$$Y = \tfrac{1}{2}\rho V^2 S C_{Y_T} \qquad M = \tfrac{1}{2}\rho V^2 S \bar{c} C_{m_T} \qquad (4)$$

$$Z = \tfrac{1}{2}\rho V^2 S C_{Z_T} \qquad N = \tfrac{1}{2}\rho V^2 S b C_{n_T}$$

where ρ represents air density, V is the velocity vector magnitude, $V = (u^2 + v^2 + w^2)^{\frac{1}{2}}$, and S, b and $\bar{c}$ denote reference area, wing span, and mean aerodynamic chord. The aerodynamic coefficients are determined by the aircraft control settings,

$$\underline{u}^T = \left[\delta_s \;\; \delta_{sp} \;\; \delta_{ds} \;\; \delta_r\right] \qquad (5)$$

which are stabilator, spoiler, differential stabilator and rudder, respectively. In addition, they are highly nonlinear functions of angle of attack and sideslip angle,

$$\alpha = \tan^{-1}(w/u) \qquad \beta = \sin^{-1}(v/V) \qquad (6)$$

The nonlinearities in (3) which were singled out in applying the new LC analysis method are $(-r \sin \phi)$, $(I_z - I_x)pr/I_y$, Z/m, N/I_z, and L/I_x. These five nonlinear terms are potentially of importance in studying lateral-mode oscillations, including possible "wing rock" mechanisms, so they were chosen for describing function treatment; the remaining terms in (3) continue to be handled by small-signal linearization. Finally, the force and moment contributions indicated above were represented as

$$\frac{Z}{m} = \frac{1}{2m}\rho V^2 S\left\{C_Z(\alpha) + \Delta C_{Z,sp}(\alpha)\frac{|\delta_{sp}|}{55} + \Delta C_{Z_{\delta_s}}(\alpha)\delta_s + \frac{\bar{c}q}{2V}C_{Z_q}(\alpha)\right\}$$

$$\frac{L}{I_x} = \frac{1}{2I_x}\rho V^2 Sb\left\{C_\ell(\alpha,\beta) + C_{\ell_{\delta_{ds}}}(\alpha)\delta_{ds} + C_{\ell_{\delta_{sp}}}(\alpha)\delta_{sp} + C_{\ell_{\delta_r}}(\alpha)\delta_r + \frac{b}{2V}\left[C_{\ell_r}(\alpha)r + C_{\ell_p}(\alpha)p\right]\right\} \tag{7}$$

$$\frac{N}{I_z} = \frac{1}{2I_z}\rho V^2 Sb\left\{C_n(\alpha,\beta) + C_{n_{\delta_{ds}}}(\alpha)\delta_{ds} + C_{n_{\delta_{sp}}}(\alpha)\delta_{sp} + C_{n_{\delta_r}}(\alpha)\delta_r + \frac{b}{2V}\left[C_{n_r}(\alpha)r + C_{n_p}(\alpha)p\right]\right\}$$

The nonlinearities given in (7) are supplied in the form of empirically determined values of the aerodynamic coefficients and stability derivatives at various flight conditions. Based on this information, the following representations were developed by curve fitting:

$$\begin{aligned}
C_Z &\cong -k_1\alpha(1-k_2\alpha^2) & C_\ell &\cong -k_{21}(1+k_{22}\alpha+k_{23}\alpha^2)\beta & C_n &\cong k_8(1-k_9\alpha)\beta \\
\Delta C_{Z,sp} &\cong k_3(1-k_4\alpha^2) & C_{\ell_{\delta_{ds}}} &\cong -k_{24}(1+k_{25}\alpha+k_{26}\alpha^2) & C_{n_{\delta_{ds}}} &\cong -k_{10}(1-k_{11}\alpha^2) \\
\Delta C_{Z_{\delta_s}} &\cong -k_5(1+k_6\alpha) & C_{\ell_{\delta_{sp}}} &\cong -k_{27}(1+k_{28}\alpha+k_{29}\alpha^2) & C_{n_{\delta_{sp}}} &\cong k_{12}(1-k_{13}\alpha) \\
C_{Z_q} &\cong -k_7\alpha & C_{\ell_{\delta_r}} &\cong k_{30}(1-k_{31}\alpha) & C_{n_{\delta_r}} &\cong -k_{14}(1-k_{15}\alpha) \\
 & & C_{\ell_r} &\cong -k_{32}(1-k_{33}\alpha) & C_{n_r} &\cong -k_{16}(1+k_{17}\alpha) \\
 & & C_{\ell_p} &= -k_{34}(1+k_{35}\alpha+k_{36}\alpha^2) & C_{n_p} &\cong -k_{18}(1+k_{19}\alpha+k_{20}\alpha^2)
\end{aligned} \tag{8}$$

To complete the nonlinear state-vector differential equation (3), the approximations

$$V = \sqrt{u^2+v^2+w^2} \cong u$$

$$\alpha = \tan^{-1}(w/u) \cong w/u \qquad (9)$$

$$\beta = \sin^{-1}(v/V) \cong v/u$$

are used in most instances. The resulting model still retains the highly nonlinear nature of the aircraft dynamics, and for k_i suitability evaluated, is realistic for the aircraft considered at angles of attack between 15 and 30 deg.

3. A NEW MULTIVARIABLE LIMIT CYCLE ANALYSIS METHOD

The need for a fresh LC analysis approach is evident from Sections 1 and 2. In summary, the existing DF methodologies based on the frequency domain cannot handle system models which realistically represent aerodynamic effects, where biases are important, and there are a number of multiple-input nonlinearities.

Before an LC analysis is undertaken, consistent input data should be specified such that an iterative technique may be used to obtain the complete equilibrium or trim condition; the values of $\underline{x}_0$ and $\underline{u}_0$ that satisfy

$$\underline{f}(\underline{x}_0, \underline{u}_0) = \underline{0} \qquad (10)$$

are determined according to (3). In a preliminary investigation of aircraft behavior for a given flight regime, small-signal linearization is useful: the (n×n) matrix F_0 defined by

$$F_0 \triangleq \left.\frac{\partial \underline{f}}{\partial \underline{x}}\right|_{\underline{x}=\underline{x}_0,\ \underline{u}=\underline{u}_0} \qquad (11)$$

determines the dynamic properties of the perturbation equation corresponding to (3). The small-signal eigenvalues, or solutions $\lambda_{0,k}$, $k = 1,2,\ldots,n$, to the characteristic equation

$$\det(\lambda_0 I - F_0) = 0 \tag{12}$$

govern the transient response of the aircraft to small perturbations for a fixed control setting, $\underline{u}(t) \equiv \underline{u}_0$.

For small α, the eigenvalues given by small-signal linearization are generally moderately well damped, and nonlinear effects may not be important. As α increases, damping generally decreases, so the nonlinear effects become critical in determining the behavior of the aircraft.

As in all SIDF analysis for limit cycle conditions, the first step is to assume that an oscillation exists in the system. For the present problem, it may be natural to assume that the steady-state angle of attack satisfies

$$\alpha = \alpha_0(1 + \kappa \sin \omega_0 t) \tag{13}$$

where α_0 is moderate and κ is generally less than unity*. The assumed frequency, ω_0, is initially the imaginary part of the most lightly damped eigenvalue given by small-signal linearization; ω_0 will be adjusted in the subsequent iterations. The goal of the limit cycle investigation is to determine either that some κ (or several values of κ) exists such that (13) is a valid assumption (limit cycles probably are present), or that no value κ can be found for which (13) is consistent with the quasi-linear system dynamic equations (limit cycles probably are not present). The describing function analysis technique developed for such a determination is iterative, and includes the following steps, which are portrayed in Fig. 2.

*Choosing the sinusoidal component amplitude to be $\kappa\alpha_0$ often leads to a convenient normalization. For limit cycle analysis about a zero center value, it would not be appropriate.

Step 0: Start the procedure with $\underline{x}_0$ from (10) and F_0 determined by small-signal linearization (11); set i = 0.

Step 1: Choose a trial value of κ in (13), e.g., $\kappa = 0.1$.

Step 2: Based on the assumed oscillation (13) and the current quasi-linear system dynamics matrix F_i, determine the amplitudes of oscillation throughout the system model by finding $\underline{a}_i$ and $\underline{b}_i$ in the steady-state solution*

$$\underline{x} = \underline{x}_i + \underline{a}_i \sin(\omega_i t) + \underline{b}_i \cos(\omega_i t) \qquad (14)$$

Step 3: Using the quasi-linear system model, determine the adjusted center $\underline{x}_{i+1}$ satisfying

$$\underline{f}_i(\underline{x}_{i+1}, \underline{u}_0) = \underline{0} \qquad (15)$$

which reflects the change from equilibrium caused by the postulated sinusoidal component of the state vector. In the same procedure, one obtains the adjusted quasi-linear system dynamics matrix $F_{i+1}(\kappa)$, which contains the sinusoidal-component describing function gains for all nonlinearities. Reset i = i+1.

Step 4: Calculate the adjusted frequency, ω_i, which is the imaginary part of the most lightly damped of the adjusted quasi-linear eigenvalues, $\lambda_{i,k}(\kappa)$,

$$\det(\lambda I - F_i(\kappa)) = 0 \qquad (16)$$

Step 5: Check to see if the iterative center determination procedure has converged;† if not, return to Step 2; if so, continue to Step 6.

Step 6: Compare $\lambda_{i,k}(\kappa)$ with eigenvalues obtained for the previous trial value of κ, denoted κ_{LAST} (in the first trial $\kappa_{LAST} = 0$, i.e., the eigenvalues are as obtained by small-signal linearization (12)):

*Determining $\underline{a}_i$ and $\underline{b}_i$ in (14) is an important step, since quasi-linear models of nonlinearities require knowing the nonlinearity input amplitudes, as is demonstrated in the next section, and it is desired to be able to treat any nonlinearity which is a function of any state variables(s).

†Steps 2 to 5 represent an iterative solution of the steady-state conditions for the bias component or "center" of the assumed oscillation; the term center is used to distinguish this point from the equilibrium $\underline{x}_0$ (10).

- If the pair of eigenvalues near the imaginary axis has crossed the axis, then some value of κ exists in the range (κ_{LAST}, κ) such that one pair of the adjusted quasi-linear eigenvalues $\lambda_{i,k}(\kappa)$ is on the imaginary axis†--a limit cycle probably exists. The value of κ, denoted κ_0, can be found by iteration on κ.

- If the pair of eigenvalues near the imaginary axis remains on the same side of the axis, increment κ (for example, by adding $\Delta\kappa = 0.1$) and repeat Steps 1 to 6.

If for a representative set of values of κ (e.g., $\kappa = 0, 0.1, 0.2, \ldots, 1.0$) the lightly damped eigenvalue pair obtained by solving (16) does not cross the imaginary axis, then it is probable that limit cycles cannot exist for the particular fixed control setting $\underline{u}_0$. Otherwise, the above procedure will iterate to find the value or values of κ which corresponds to probable limit cycle amplitudes.

Some comments and details about the procedures mentioned in Steps 2 and 3 are in order, since they are central to the new technique. First, consider the problem of obtaining $\underline{a}_i$ and $\underline{b}_i$ in (14): Given the adjusted equilibrium and quasi-linear system dynamics matrix that are known from the previous iteration, $\underline{x}_i$ and F_i, plus an assumed oscillation in one state,

$$x_k = a_k \sin(\omega_i t)$$

(neglecting the bias component), it is desired to determine the complex vector of amplitudes, $\underline{a}^*$, such that $\underline{x} = \underline{a}^* \sin \omega_i t$. The use of the complex amplitude vector $\underline{a}^*$ corresponds to the standard phasor representation, $\underline{a}^* = \underline{a}_i + j\underline{b}_i$. If ω_i is a natural frequency corresponding to $\dot{\underline{x}} = F_i\underline{x}$, then

†This condition corresponds to satisfying (2) for some value of $a_0 = \kappa\alpha_0$.

$$(j\omega_i I - F_i)\underline{a}^* \triangleq M^*(\omega_i)\underline{a}^* = \underline{0} \qquad (17)$$

The latter relation serves to define the entire vector $\underline{a}^*$, given one of its elements, a_k, by deleting one scalar relation and solving the remaining (n-1) equations. This approach is dealt with in some detail in [13, 14].

The solution $\underline{a}^*$ for specified a_k is not unique unless ω_i is, in fact, an eigenvalue of F_i. This will be true only for a value of κ for which limit cycles are predicted -- i.e., the algorithmic technique should converge to such a situation, but is will not generally be initialized with (17) satisfied for F_0. The amplitude vector, $\underline{a}^*$, contains useful information as to the coupling of the oscillation into all of the states. This data is approximately equivalent to that conveyed by eigenvectors, becoming exact when $j\omega_i$ is an eigenvalue of F_i.

The nonlinearities given in (3-9) involve many multiple-input terms. The general SIDF format is then

$$f \cong f_0(\underline{x}_i, \underline{a}_i, \underline{b}_i) + \sum_{j=1}^{n} n_j(\underline{x}_i, \underline{a}_i, \underline{b}_i)\cdot(a_{j,i}\sin\omega_i t + b_{j,i}\cos\omega_i t)$$

where f_0 and n_j, j=1,n are the describing function gains. The SIDF term f_0 for each nonlinearity thus appears in the quasi-linear system equation for the adjusted center (15), and each gain n_j is used in evaluating the quasi-linear system dynamics matrix F_i(16). In many instances the nonlinear relations incorporate powers of state variables; as in example, the SIDF approximation for $x_1 x_2^3$ where x_1 and x_2 are arbitrary state variables is

$$x_1 x_2^3 = \left[x_{1,i} x_{2,i}^3 + \frac{3}{2} x_{2,i}\left(x_{1,i} r_{22} + x_{2,i} r_{12}\right) + \frac{3}{8} r_{12} r_{22}\right]$$

$$+ \left[x_{2,i}^3 + \frac{3}{4} x_{2,i} r_{22}\right] \cdot \left(a_{1,i} \sin \omega_i t + b_{1,i} \cos \omega_i t\right)$$

$$+ \left[3x_{1,i} x_{2,i}^2 + \frac{3}{4} x_{1,i} r_{22} + \frac{3}{2} x_{2,i} r_{12}\right] \cdot \left(a_{2,i} \sin \omega_i t + b_{2,i} \cos \omega_i t\right)$$

where

$$r_{jk} = a_{j,i}\, a_{k,1} + b_{j,i} b_{k,i} \quad ; \quad j,k=1,2$$

SIDF representations for any power series term can be obtained quite simply as follows: substitute for each state variable according to (14), multiply out, apply suitable trigonometric identities to reduce the expression to fourier series form (i.e., all powers of trigonometric functions are reduced to bias plus fundamental plus higher harmonic terms), and retain only the bias and fundamental components.

4. APPLICATION OF THE MULTIVARIABLE LIMIT CYCLE ANALYSIS METHOD

The aerodynamic data curve fits obtained by adjusting the coefficients k_1 through k_{36} in (8) were initially verified by plotting the Dutch roll eigenvalue real part, obtained by small-signal linearization, versus the trim value of angle of attack. The curve, shown in Fig. 3, reflects the observation that the Dutch roll mode stability boundary given by direct partial differentiation of the experimental aerodynamic data is very close to 20 deg ($\alpha \cong 19.6$ deg). This case ($\alpha = 19.6$ deg) corresponds to the nearly straight-and-level flight condition specified in Table 1; the corresponding control setting $\underline{u}_0$ was therefore chosen for study since small-signal linearization leads to nearly marginal stability and higher-order nonlinear terms thus become critical in determining the aircraft

performance. The corresponding eigenvalues associated with the Dutch roll mode are

$$\lambda_{DR} = 0.0366 \pm 1.52j$$

which for small perturbations predicts an unstable response. It should be observed that there is a much slower unstable lateral mode ("lateral phugoid"), with eigenvalues

$$\lambda_{LP} = 0.0187 \pm 0.131j$$

In most instances, a mode which is as slow as the lateral phugoid in the present case is not a concern, so attention is generally restricted hereafter to the behavior of the Dutch roll mode.

The search for possible limit cycles was conducted by assuming that the velocity along the body y-axis is given by

$$v = v_o \left[1 + \kappa \sin(\omega_{DR} t)\right]$$

where ω_{DR} is the imaginary part of the lightly damped Dutch roll mode. The parameter κ was varied from 0 to 3 in steps of 0.5; the resulting change in $\lambda_{DR}(\kappa)$ is shown in Fig 4. Based on these results, limit cycles for κ between 1 and 1.5 and for κ between 2.5 and 3.0 are anticipated. The smaller LC is predicted to be stable according to the usual SIDF argument [1-4], while the larger unstable limit cycle prediction is of no practical interest, because it is beyond the region where the curve fits in (8) are realistic.

The multivariable LC analysis program was then permitted to iterate to find the exact limit cycle condition. It was found that λ_{DR} is virtually on the imaginary axis,

$$\lambda_{i,DR} = 4\times10^{-5} \pm 1.495j$$

for κ equal to 1.20. Corresponding to this value of κ, the "center" value $\underline{x}_i$ and oscillation components $\underline{a}_i$ and $\underline{b}_i$ for the state vector are given in Table 2.

Checking the limit cycle prediction requires that nonlinear simulations of the dynamics specified in (3-9) be performed. To do this, the state equation (3) is recast as

$$\dot{\underline{x}} = F_1\underline{x} + \begin{bmatrix} -r\sin\phi \\ 0 \\ (I_z-I_x)pr/I_y \\ Z/m \\ 0 \\ N/I_z \\ L/I_x \\ 0 \end{bmatrix} + G_1\underline{u} \triangleq F_1\underline{x} + \underline{f}_1(\underline{x},\underline{u}) + G_1\underline{u} \qquad (18)$$

where F_1 and G_1 are constant matrices which capture effects other than those chosen for study via quasi-linearization, and $\underline{f}_1(\underline{x},\underline{u})$ contains the nonlinearities selected for SIDF treatment. Equation (18) can then be integrated to yield the desired time histories.

Choice of the initial condition for this procedure is critical. This is a due to the presence of an unstable mode, a slow spiral mode which for $\kappa = 1.2$ is governed by $\lambda_S = 0.0618$. If this mode is excited appreciably, its growth will completely obscure the fast limit cycle that is sought. One of the benefits of the new LC analysis method is that the eigenvector for the predicted limit cycle is $\underline{a}_i + j\underline{b}_i$; therefore, if we choose the initial condition $\underline{x}(0) \cong \underline{a}_i$ only the limit cycle in the Dutch roll mode should be excited appreciably.

The stable limit cycle prediction shown in Table 2 was verified by choosing $\underline{x}(0) = 0.8\underline{a}_i$. The resulting time histories of pitch angle θ, y body-axis velocity v, and z body-axis velocity w, are portrayed in Fig. 5*. The plot of θ shows that the solutions do diverge very slowly, due to a small unavoidable excitation of the spiral mode. The time histories of v and w show that the dominant Dutch roll mode is very slowly growing for the first 25 sec of the simulation, as would be expected for an initial condition that is slightly interior to the predicted stable limit cycle. The predicted center value of v is nearly exact, while that for w is in error by about -0.5 m/sec, or about -1.4 percent. Finally, the predicted limit cycle frequency is 1.495 rad/sec, while the observed frequency is 1.497 rad/sec; the agreement is excellent. After 25 sec of simulation, the slow divergence begins to alter the limit cycle that developed in the first part.

Further analysis of the simulation results was undertaken to attempt to separate out the effect of the slow divergence. The time history depicted in Fig. 5b was processed to determine the exponential growth component ($c_1 e^{c_2 t}$); then the predicted limit cycle envelope is given by the relation

$$e_{LC} = c_1 e^{c_2 t} \pm a_5$$

where a_5 is the amplitude of the predicted limit cycle in v (state 5). This envelope is portrayed in Fig. 5b; within the limits of the simulation accuracy, convergence of the time history to the envelope is shown.

The effort to verify the limit cycle condition by direct simulation has pointed up the difficulty of using

*The plots show the perturbation of each variable about the predicted center value, $\underline{x}_i$.

the latter technique as an exploratory tool to locate limit cycles, without recourse to describing function analysis. Realistic aerodynamic models such as those used here often have slow modes that are unstable or that are very lightly damped. Direct simulation initial conditions must be chosen very carefully to avoid exciting these modes. In a linear system, it is not difficult to use eigenvector information to obtain initial conditions that selectively excite a desired mode. However, eigenvectors are not rigorously defined for nonlinear systems.

A concept which has been used with some success may be called the quasi-linear eigenvector; in essence, the complex vector $\underline{a}^*$, given by $\underline{a}_i + j\underline{b}_i$ as in Table 2, is in a sense an amplitude-dependent eigenvector, which specifies an initial condition that excites the predicted oscillation. The fact that the quasi-linear eigenvector $\underline{a}^*$ is amplitude-dependent is illustrated in Fig. 6, which shows $\underline{a}^*$ for various values of κ, corresponding to the study depicted in Figs. 4 and 7†. For κ = 1.0 and 1.5, the eigenvector components for θ and q are too small to be shown; the differences between the remaining components (which are normalized to make the length of the v component equal in each plot) are rather small. For κ = 2.5 and 3.0, the changes in $\underline{a}^*$ are quite substantial. For example, the θ and q components of $\underline{a}^*$ are much larger than for small κ, and can be seen to rotate nearly 45 deg for κ increased from 2.5 to 3.0.

†The eigenvectors correspond to the variables θ, u, q, w, v/10, r, p/5, ϕ/5; this scaling was performed to permit all components of $\underline{a}^*$ to be shown on the plots for κ=2.5 and 3.0.

5. SUMMARY AND CONCLUSIONS

The SIDF technique described in this paper (and in [13-15]) permits the investigation of LC conditions in completely general multivariable nonlinear systems; restrictions as to the type and number of nonlinearities, and the system configuration, have been completely removed. Since a general state variable system formulation is used throughout the analysis, there is no need to manipulate a system model into the form of linear dynamics in the forward path and nonlinearities in the feedback path, as in Fig. 1.

Naturally, the usual SIDF caveat must be kept in mind: The inputs to all nonlinearities must be reasonably approximated by the form bias-plus-sinusoid. The general state-space formulation of the problem deprives the analyst of the more concrete alternative statement of this warning, viz. "the linear dynamics (W(s)) must be low-pass and the nonlinearities must not produce output signals with undue higher harmonic content"; however, for high-order systems with a number of nonlinearities, it is not at all clear how meaningful such a statement might be. It is fair to say that using any SIDF technique in this context requires some experience, based on either simulation or direct observation of the system being analyzed, which can provide some assurance that the assumed nonlinearity input form is reasonable (e.g., see Fig. 5).

A major point of departure from previous SIDF analysis methods is the substitution of root locus-like plots of "quasi-linear eigenvalues" in lieu of frequency-response plots based on $W(j\omega)$; this alternative viewpoint has permitted the breakthrough in terms of system model generality in comparison with frequency-domain/SIDF techniques for multivariable systems [5-11]. As a result, one loses the ability to modify or remove

LC conditions by the classical methods for altering the frequency response of W(s) by changing pole locations or adding "compensation networks". However, systems designers versed in the more modern technique of pole placement using state variable feedback should find that method of system response compensation applicable to LC conditions found using this new SIDF technique; an approach due to Sankaran (16) appears to be particularly useful in this regard. Combining the new SIDF LC analysis method with an iterative pole position modifying algorithm would result in a very powerful approach to multivariable nonlinear systems synthesis.

The study presented in Section 4 illustrates the effectiveness of the new LC analysis method. The predicted LC frequency and "center" value (Fig. 5) are in good agreement with the simulation results; the accuracy of the amplitude prediction is more difficult to assess quantitatively due to the simulation problems mentioned previously (see Fig. 5b). In general, these results bolster the expectation that the new iterative LC analysis technique will be found to converge to locate limit cycle conditions, provided that

- The input equilibrium condition specification leads to a pair of small-signal linear eigenvalues that are lightly damped
- The nonlinearities are well-behaved (e.g., realistically modeled by low-order power series expansions or products thereof)
- Limit cycles indeed exist (as verified by simulating solutions to the original nonlinear state-vector differential equation, with suitable initial conditions)

Considerable further research should be performed to conclusively prove the power and accuracy of the new SIDF LC analysis approach. As a first step, it would be valuable to

apply it to a simpler model (fewer states and nonlinearities), particularly one that does not contain system variables that are slowly divergent. The existence of unstable modes, or even of modes that are slowly decaying oscillations, makes limit cycle verification by direct simulation very difficult, since it is impossible not to excite them in the simulation.

Finally, the primary benefits of this technique are

- An iterative algorithmic approach to limit cycle analysis is much more suitable for mechanization on a digital computer than classical frequency-domain techniques, which are typically graphical in nature;
- Any number of nonlinear effects can be investigated, singly or in any combination, without continually manipulating the system model into the appropriate "linear plant with nonlinear feedback" formulation required in the frequency-domain approach (Fig. 3);
- The amount of computer time required to determine the existence of limit cycles by the new SIDF approach should generally be significantly less than the computer time expenditure that would be needed using direct simulation alone.

The last observation is based on the difficulty of choosing the direct simulation initial condition correctly to excite only the desired nearly oscillatory mode, as discussed in the preceding section.

REFERENCES

1. Gibson, J.E., Nonlinear Automatic Control, McGraw-Hill, New York, 1963.

2. Gelb, A. and Vander Velde, W.E., Multiple-Input Describing Functions and Nonlinear System Design, McGraw-Hill, New York, 1968.

3. Hsu, J.C. and Meyer, A.U., Modern Control Principles and Applications, McGraw-Hill, New York, 1968.

4. Atherton, D.A., Nonlinear Control Engineering, Van Nostrand Reinhold, New York, 1975.

5. Ramani, N. and Atherton, D.P., "Stability of Nonlinear Multivariable Systems," Proc. Canadian Automatic Control Conference, 1973.

6. Mees, A. "Describing Functions, Circle Criteria and Multiple-Loop Feedback Systems," Proc. IEE, Vol. 120, No. 1, Jan. 1973. (See also the comment on this paper, by Ramani, N. and Atherton, D.P., Proc. IEE, Vol. 120, No. 7, July 1973.)

7. Gran, R. and Rimer, M. "Stability Analysis of Systems with Multiple Nonlinearities," IEEE Trans. on Automatic Control, Vol. AC-9, No. 1, Jan. 1965.

8. Lee, R. and Clark, L.G., "Analysis and Compensation of Systems Containing Multiple Nonlinearities," ASME 89th Winter Annual Meeting, New York, December 1968.

9. Garg, D.P. and Aleman, R., "A Limit Cycle Analysis of Control Systems with Multiple Non-Linearities, "Intl. J. of Control, Vol. 16, No. 5, May 1972.

10. Jud, H.G., "Limit Cycle Determination for Parallel Linear and Nonlinear Elements," IEEE Trans. on Automatic Control, Vol. AC-9, No. 2, April 1964.

11. Hopkins, W.G., III, "On the Prediction of Limit Cycles in Systems Containing Multiple Nonlinearities," Proc. IEEE Southwestern Conference, April 1973.

12. Etkin, B., Dynamics of Atmospheric Flight, John Wiley, New York, 1972.

13. Taylor, J.H., "An Algorithmic State-Space/Describing Function Technique for Limit Cycle Analysis," IOM, The Analytic Sciences Corporation (TASC), Reading, Massachusetts, April 1975. (Also issued as TASC TIM-612-1 to the Office of Naval Research, Oct. 1975).

14. Taylor, J.H., et al, "High Angle of Attack Stability and Control," Office of Naval Research Report ONR-CR215-237-1, April 1976.

15. Taylor, J.H., "A New Algorithmic Limit Cycle Analysis Method for Multivariable Systems," TIM-612-2, TASC, Reading, Massachusetts, Oct. 1977.

16. Sankaran, V., "An Iterative Technique to Stabilize a Linear Constant System," IEEE Trans. on Automatic Control, Vol. AC-20, No. 2, April 1975.

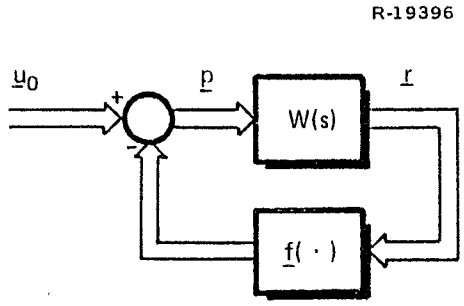

Figure 1 A System Model With Multiple Nonlinearities

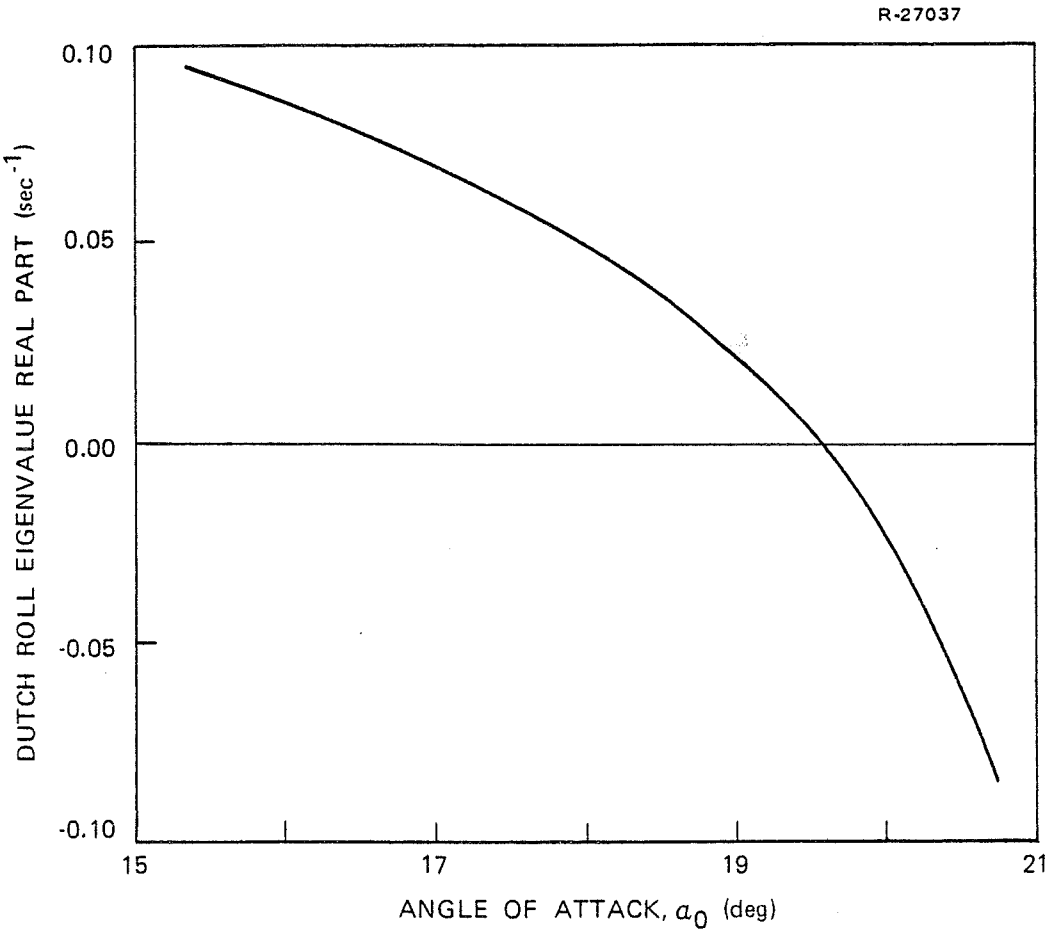

Figure 3 Dutch Roll Eigenvalue Real Part as Determined by Trim Angle of Attack

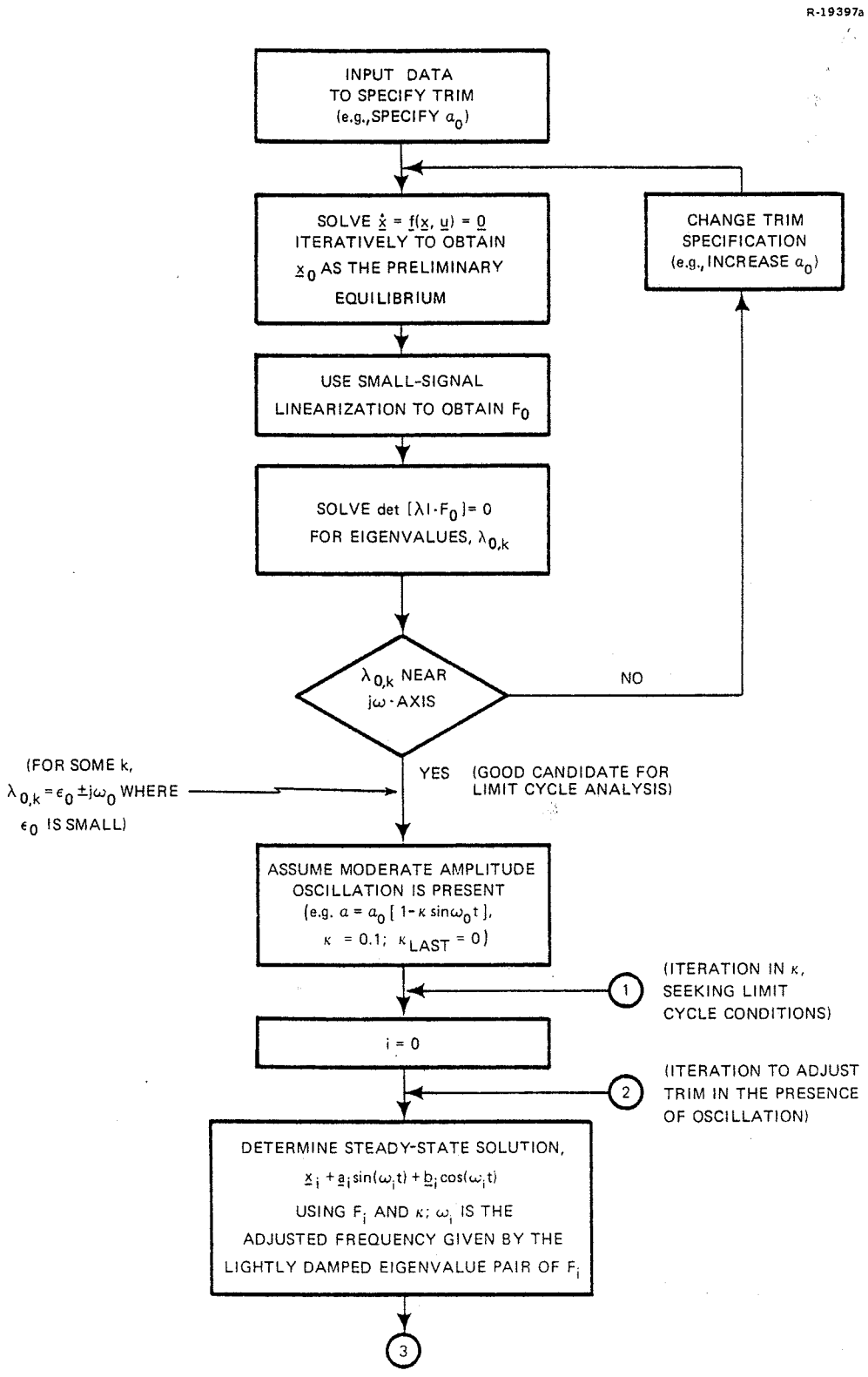

Figure 2 Iterative Search Technique for Limit Cycles -- The Multivariable Limit Cycle Analysis Technique (Sheet 1 of 2)

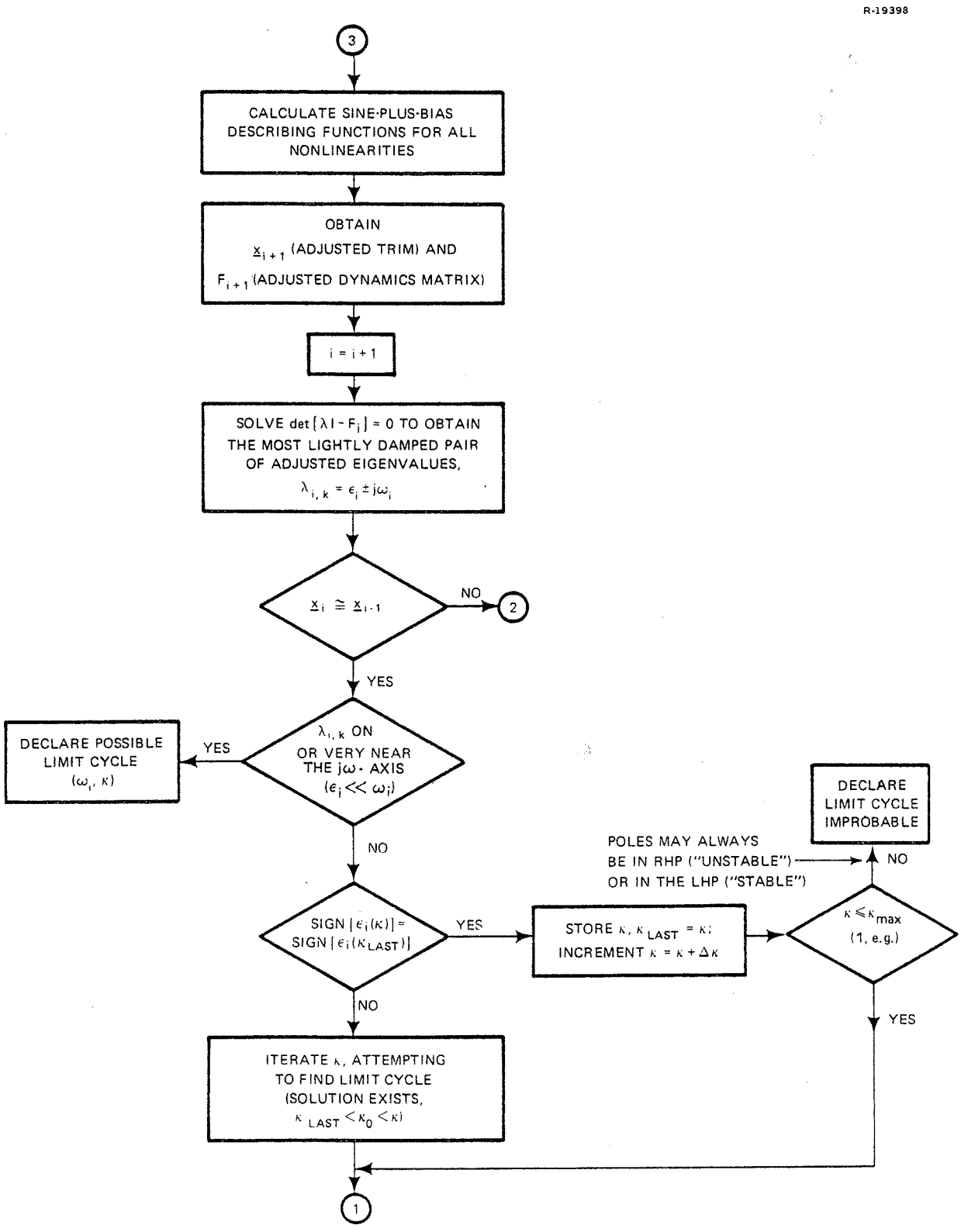

Figure 2 Iterative Search Technique for Limit Cycles -- The Multivariable Limit Cycle Analysis Technique (Sheet 2 of 2)

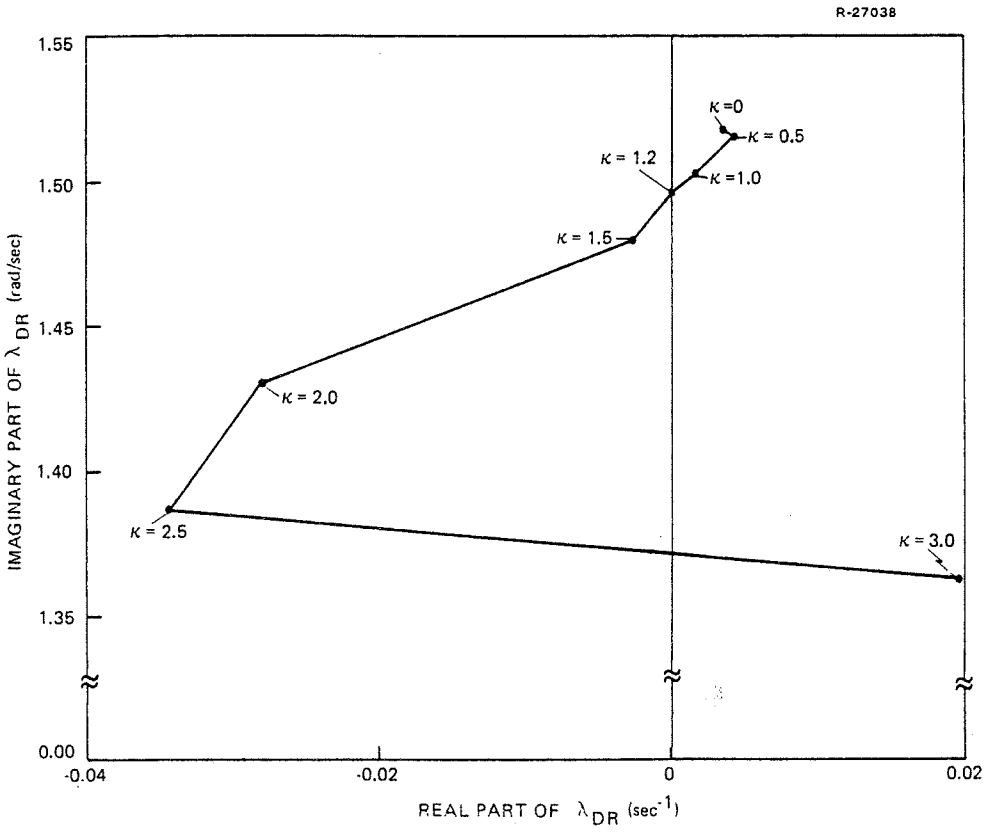

Figure 4 Variation of the Dutch Roll Eigenvalue With Assumed Oscillation Amplitude

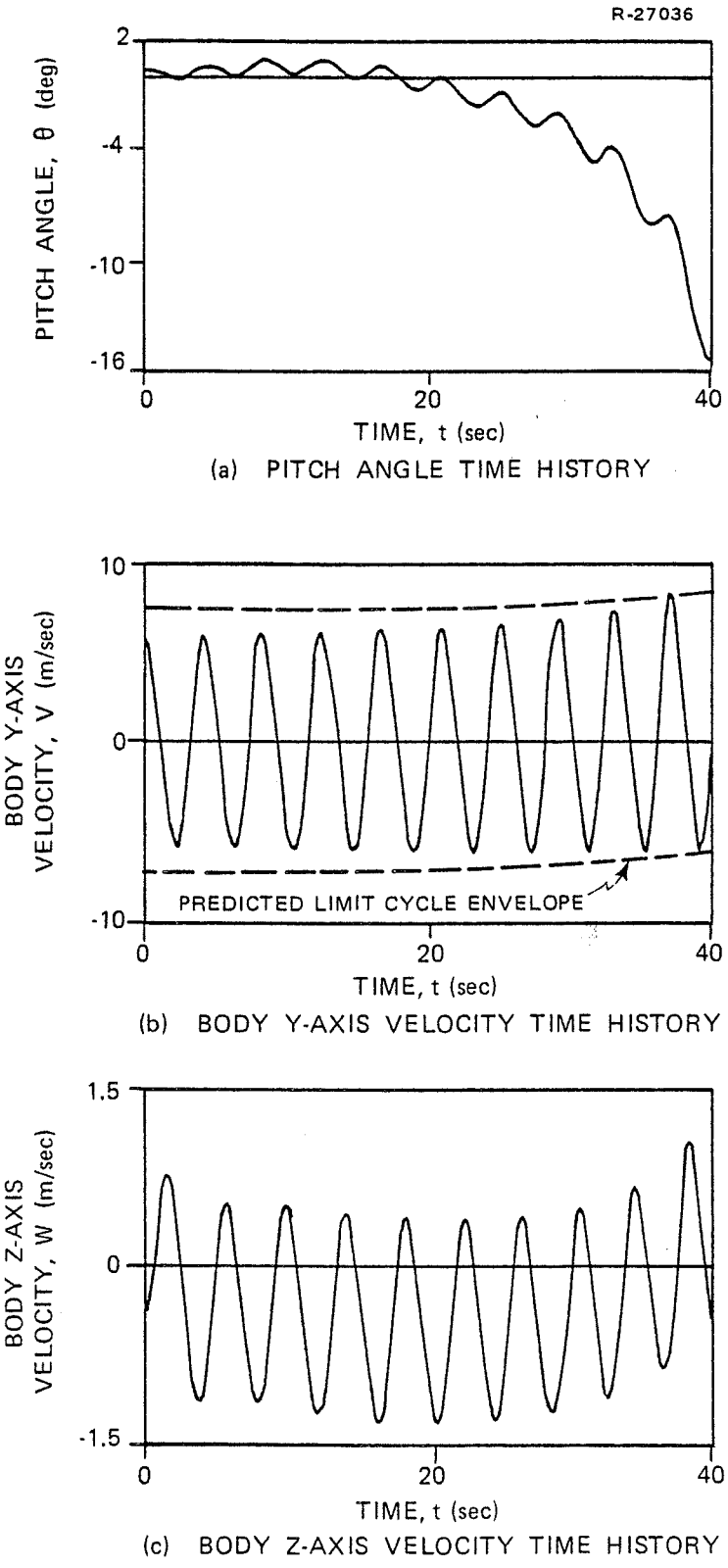

Figure 5 Verification of the Limit Cycle Prediction

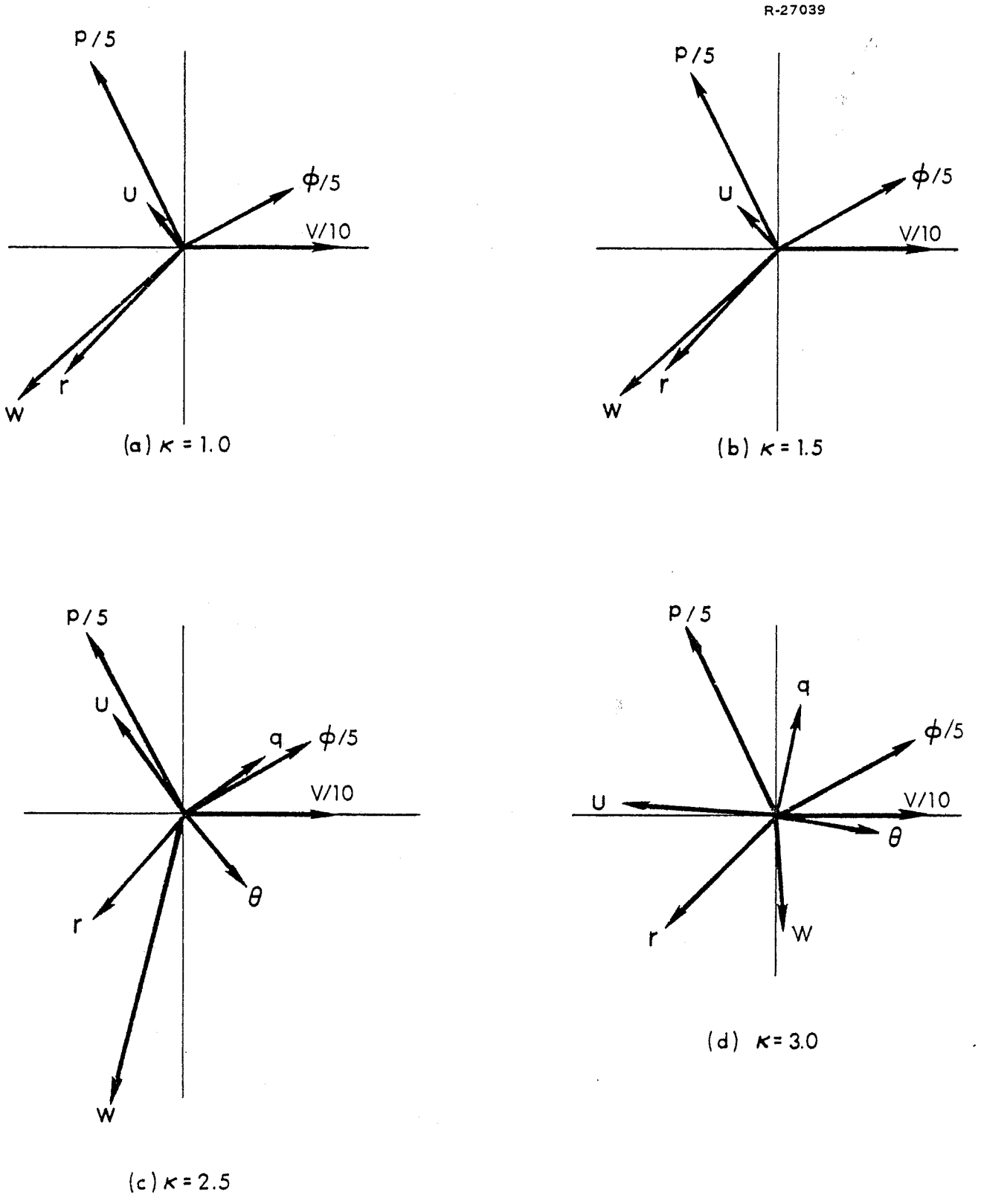

Figure 6 Amplitude Dependence of Quasi-Linear Eigenvectors

TABLE 1

SELECTED EQUILIBRIUM CONDITION IN THE ABSENCE OF OSCILLATION

T-1435

STATE VARIABLE (ELEMENT OF $\underline{x}_0$)	VALUE
θ_0	17.46 deg
u_0	81.7 m/sec
q_0	0.296 deg/sec
w_0	29.1 m/sec
v_0	6.04 m/sec
r_0	-0.033 deg/sec
p_0	-0.011 deg/sec
ϕ_0	-5.303 deg

TABLE 2

CENTER CONDITION AND PREDICTED LIMIT CYCLE AMPLITUDE FOR THE STABLE LIMIT CYCLE

T-1436

STATE VARIABLE CENTER (ELEMENT OF $\underline{x}_i$)		$\underline{a}_i$	$\underline{b}_i$	UNITS
θ_i	18.35	0.259	-0.234	deg
u_i	80.25	-0.177	0.165	m/sec
q_i	0.174	0.219	0.182	deg/sec
w_i	28.80	-0.810	-0.718	m/sec
v_i	6.14	7.38	0.0	m/sec
r_i	0.792	-1.79	-1.89	deg/sec
p_i	-0.310	-7.35	14.90	deg/sec
ϕ_i	8.55	9.55	5.295	deg

FIGURE AND TABLE CAPTIONS